Immune complex solubility and size govern Fc-gamma receptor responses: A scalable cell-based reporter system

Haizhang Chen[1,2], Andrea Maul-Pavicic[3,4], Martin Holzer[5], Ulrich Salzer[3], Nina Chevalier[3], Reinhard E. Voll[3,4], Hartmut Hengel[1,2,*] & Philipp Kolb[1,2,*]

[1]Institute of Virology, University Medical Center, Albert-Ludwigs-University Freiburg, Hermann-Herder-Str. 11, 79104 Freiburg, Germany

[2]Faculty of Medicine, Albert-Ludwigs-University Freiburg, 79104 Freiburg, Germany

[3]Department of Rheumatology and Clinical Immunology, Medical Center - University of Freiburg, Faculty of Medicine, University of Freiburg, Hugstetterstr. 55, 79106 Freiburg, Germany

[4]Center for Chronic Immunodeficiency (CCI), Medical Center-University of Freiburg, Faculty of Medicine, University of Freiburg, Breisacherstr. 115, 79106 Freiburg, Germany

[5]Institute for Pharmaceutical Sciences, Albert-Ludwigs-University Freiburg, Hermann-Herder-Str. 9, 79104 Freiburg, Germany

*corresponding authors (Hartmut.hengel@uniklinik-freiburg.de)

One Sentence Summary: This study reveals selective activation of individual Fc-gamma receptors by soluble but not immobilized immune complexes, establishing a novel biomarker for autoimmune disease in humans and mouse models.

Abstract: Fc-gamma receptor (FcγR) activation by soluble IgG immune complexes (sICs) is thought to be a major mechanism of inflammation in certain autoimmune diseases such as systemic lupus erythematosus (SLE). A robust and scalable test system allowing for the detection and quantification of sIC bioactivity is missing. Therefore, we developed a comprehensive reporter cell panel capable of measuring the sIC-mediated activation of individual human and mouse FcγRs. We show that compared to human FcγRs IIB and III, human FcγRs I and IIA lack sensitivity to sICs. Further, the assay proved to be sensitive to sIC stoichiometry and size enabling us to demonstrate for the first time a complete translation of the Heidelberger-Kendall precipitation curve to FcγR responsiveness. This was validated using primary immune cells. The approach was applied to quantify sIC-mediated FcγR activation using sera from SLE patients or from mouse models of lupus and arthritis. Thus, in clinical practice, it can be employed as a toolbox enabling the evaluation of FcγR activation by sICs as a biomarker for disease activity in immune-complex mediated diseases.

Introduction

Immunoglobulin G (IgG) is the dominant immunoglobulin isotype in chronic infections and in antibody-mediated autoimmune diseases. The multi-faced effects of the IgG molecule rely both on the F(ab) regions, which recognize a specific antigen to form immune complexes (ICs), and the constant Fc region (Fcγ), which is detected by Fcγ receptors (FcγRs) found on most cells of the immune system (*1*). When IgG binds to its antigen ICs are formed, which, depending on the respective antigen, are either cell-bound or soluble (sICs). The composition of sICs is dependent on the number of epitopes recognized by IgG on a single antigen molecule and the ability of the antigen to form multimers. Fcγ-FcγR binding is necessary but not sufficient to activate FcγRs since physical receptor cross-linking generally underlies receptor activation (*2-5*). Firmly fixed cell bound ICs are readily able to cross-link FcγRs (*4, 6*). This condition induces various signaling pathways (*7-9*) which in turn regulate immune

51 cell effector functions (*10, 11*). It is also suggested that sICs can dynamically tune FcγR
52 triggering, implying that changes in sIC size directly impact FcγR responses (*6*). However,
53 the molecular requirements are largely unknown. Also, a functional reproduction of the
54 paradigmatic Heidelberger-Kendall precipitation curve, describing that the molecular size of
55 sICs determined by the antibody:antigen ratio dynamically tunes FcγR activation on and off
56 (*12, 13*), is so far missing.
57 In contrast to FcγR binding of monomeric ligands without consequences, IC-mediated FcγR
58 cross-linking initiates the full signal cascade followed by immune cell activation or inhibition,
59 resp. (*5, 8, 14, 15*). Human FcγRs are membrane resident receptors recognizing Fcγ. Among
60 all type I FcγRs, FcγRIIB (CD32B) is the only inhibitory one signaling via immunoreceptor
61 tyrosine-based inhibitory motifs (ITIMs) while the activating receptors are associated with
62 immunoreceptor tyrosine-based activation motifs (ITAMs). Another exception is FcγRIIIB
63 (CD16B), which is glycosylphosphatidylinositol (GPI)-anchored (*16-19*). FcγRI (CD64) is the
64 only receptor with high affinity binding to monomeric IgG not associated with antigen and is
65 primarily tasked with phagocytosis linked to antigen processing and pathogen clearance (*20,*
66 *21*). All the other FcγRs only efficiently bind to complexed, meaning antigen-bound IgG (*1,*
67 *16, 17*). While FcγRI, FcγRIIB and FcγRIIIA are able to recognize sICs, this has not been
68 reported for FcγRIIA (CD32A), rather this receptor has recently been shown to depend on the
69 neonatal Fc receptor (FcRn) or FcγRIIIB (CD16B) to do so (*22, 23*). Activation of FcγRs
70 leads to a variety of cellular effector functions such as antibody-dependent cellular
71 cytotoxicity (ADCC) by natural killer (NK) cells via FcγRIIIA, antibody-dependent cellular
72 phagocytosis (ADCP) by macrophages via FcγRI, cytokine and chemokine secretion by NK
73 cells and macrophages via FcγRIIIA. Further effector responses are reactive oxygen species
74 (ROS) production of neutrophils and neutrophil extracellular traps formation (NETosis) via
75 FcγRIIIB, dendritic cell (DC) maturation and antigen presentation via FcγRIIA and B cell
76 selection and differentiation via FcγRIIB (*10, 24-30*). Consequently, FcγRs connect and

77 regulate both innate and adaptive branches of the immune system. Various factors have been
78 indicated to influence the IC-dependent FcγR activation profiles, including Fcγ-FcγR binding
79 affinity and avidity (*31*), IgG subclass, glycosylation patterns and genetic polymorphism (*4,*
80 *24, 25, 32*), stoichiometry of antigen-antibody-ratio (*6, 30, 33*) and FcγR clustering patterns
81 (*34*). Specifically, Asn297-linked glycosylation patterns of the IgG Fc domain initiate either
82 pro- or anti-inflammatory effector pathways by tuning the binding affinity to activating versus
83 inhibitory FcγRs, respectively (*35*). However, despite being explored in proof-of-concept
84 studies, the functional consequences of these ligand features on a specific receptor are still not
85 fully understood. Therefore, an assay platform allowing for the systematic functional
86 assessment of IC-mediated FcγR activation is strongly required. While a previously
87 developed cell-based assay addresses sIC-mediated activation of the inhibitory FcγRIIB (*36*),
88 a platform allowing for the comprehensive analysis of all FcγRs is missing.
89 sICs and immobilized ICs represent different stimuli for the immune system (*22, 29*). Soluble
90 circulating ICs are commonly associated with certain chronic viral or bacterial infections (*37,*
91 *38*) and autoimmune diseases, such as systemic lupus erythematosus (SLE) or rheumatoid
92 arthritis (RA) (*39-41*). When accumulating and deposited in tissues sICs can cause local
93 damage due to inflammatory responses, classified as type III hypersensitivity (*42*). Typically,
94 sICs related disorders are characterized by systemic cytokine secretion which can be followed
95 by immune cell exhaustion and senescence (*43, 44*). In order to study sIC-dependent
96 activation of FcγRs in detail, we employed a cell-based assay which has been previously
97 utilized to study immobilized ICs (*45*) and adapted it into a sIC sensitive reporter system
98 capable of distinguishing the activation of individual FcγRs and their responses to varying
99 complex size. This approach allowed for the first time a complete reproduction of the
100 Heidelberger-Kendall precipitation curve measuring actual FcγR triggering. The assay
101 enables a quantification of clinically relevant sICs in sera from SLE patients and autoimmune-

102 prone mice with immune-complex-mediated arthritis and lupus using reporter cells expressing
103 chimeric mouse FcγRs.
104
105 **Results**
106 *Experimental assay setup*
107 The assay used in this study was adapted from a previously described cell-based FcγR
108 activation assay designed to measure receptor activation in response to opsonized virus
109 infected cells (*45*) or therapeutic Fc-fusion proteins (*46*). We complemented the assay setup to
110 enable measurement of sICs when incubated with reporter cells stably expressing the
111 ectodomains of the human FcγR fused to the signaling module of the mouse CD3-ζ chain
112 (FcγRI: Acc# X14356; FcγRIIA(R): Acc# X62572; FcγRIIB/C: Acc# X52473; FcγRIIIA(V):
113 Acc# LT737365). Ectodomains of FcγRIIB and FcγRIIC are identical. Second generation
114 reporter cells were generated to improve stable expression of chimeric FcγRs compared to the
115 transfectants used in the original assay (*45*). To this end, BW5147 cells were transduced as
116 described previously via lentiviral transduction (*45, 47*). Human FcγR expression on
117 transduced cells after puromycin selection is shown in Fig. 1A. FcγR triggering is translated
118 into activation of the reporter cells and measured by quantification of endogenous IL-2 (mIL-
119 2) secretion into the cell culture supernatant using an anti-IL-2 sandwich ELISA as described
120 previously (*45*). In order to employ the original assay, designed to detect ICs on adherent
121 virus-infected cells, for the detection of soluble ICs we first determined the suspension of IgG
122 achieved by pre-incubating a 96 well ELISA microtiter plate with PBS/FCS blocking buffer.
123 To this end, we compared graded concentrations of FCS in the blocking reagent and measured
124 the threshold at which IgG (rituximab, Rtx) was no longer adsorbed to the plate and stayed
125 abundantly in solution. Fig. 1B demonstrates that FCS supplementation to 1% (v/v) or higher
126 is sufficient to keep IgG antibodies in solution and prevents binding to the plastic surface.
127 Using this adapted protocol, the assay now allowed for the sensitive detection and

128 characterization of FcγR interaction with immobilized ICs versus sICs as shown
129 schematically in Fig. 1C. First, we set out to test if monomeric IgG upon immobilization
130 becomes an operational surrogate for IgG-opsonized cells or immobilized ICs with regard to
131 FcγR activation as suggested before (*48*). As depicted in Fig. 2, there was no qualitative
132 difference in FcγR activation between immobilized Rtx, immobilized ICs (Rtx + rec. CD20)
133 or Rtx-opsonized 293T-CD20 cells, showing that FcγR cross-linking by clustered IgG alone is
134 sufficient for receptor cross-linking and activation. In contrast, sICs formed by monomeric
135 CD20 peptide (aa 141-188) and Rtx failed to activate FcγRs even at very high ligand
136 concentrations. Based on this finding we hypothesized that, in order to generate sICs able to
137 activate FcγRs, antigens have to be multivalent to achieve cross-linking of FcγRs. Of note, to
138 reliably and accurately differentiate between soluble and immobilized triggers using this
139 assay, reagents for the generation of ICs need to be of very high purity and consistent
140 stability. Indeed, only combinations of pharmaceutical therapy grade, i.e. ultra-pure mAbs and
141 pure antigens (purified via size exclusion chromatography) showed reproducible, dose-
142 dependent and specific activation in the reporter assay (data not shown).
143
144 *Quantification of human FcγR responsiveness to multimeric sICs*
145 To date, there are only few commercially available human IgG-antigen pairs that meet both
146 the above mentioned high grade purity requirements while also providing a multimeric
147 antigen. In order to meet these stipulations of ultra-pure synthetic soluble immune complexes
148 we focused on three pairs of multivalent antigens and their respective mAbs that were
149 available in required amounts enabling large-scale titration experiments; trimeric
150 rhTNFα:IgG1 infliximab (TNFα:Ifx), dimeric rhVEGFA: IgG1 bevacizumab (VEGFA/Bvz)
151 and dimeric rhIL-5: IgG1 mepolizumab (IL-5/Mpz). As lymphocytes express TNFα-receptors
152 I and II while not expressing receptors for IL-5 or VEGFA, we tested whether the mouse
153 lymphocyte derived BW5147 thymoma reporter cell line is sensitive to high concentrations of

154 rhTNFα. Toxicity testing revealed that even high concentrations up to 76.75 nM rhTNFα did
155 not affect viability of reporter cells (Fig. S1). Next, we measured the dose-dependent
156 activation of human FcγRs comparing immobilized IgG to soluble ICs using the FcγR
157 reporter cell panel (Fig. 3). Soluble antigen or mAb alone served as negative controls showing
158 no background activation even at high concentrations. Immobilized rituximab served as a
159 positive control for inter-experimental reference. We observed that all FcγRs are strongly
160 activated in a dose-dependent manner when incubated with immobilized IgG. Incubating the
161 FcγR reporter cells with sICs at identical molarities showed FcγRIIB/C and FcγRIIIA to be
162 efficiently activated by sICs, while in contrast, FcγRIIA and FcγRI did not respond to sICs.
163 We furthermore observed FcγRIIIA to be efficiently activated by sICs with responses even
164 surpassing those achieved with immobilized IgG for TNFα/Ifx and IL-5/Mpz ICs. FcγRIIB/C
165 showed a generally weaker reactivity towards sICs compared to immobilized ICs, especially
166 at high concentrations whereas an inversion of this order was seen for TNFα/Ifx and
167 VEGFA/Bvz ICs at lower concentrations. IL-5/Mpz, FcγRIIB/C and FcγRIIIA showed
168 similar responsiveness towards immobilized or sICs with a generally stronger activation on
169 immobilized ICs. These findings demonstrate that sICs of different composition vary in the
170 resulting FcγR activation pattern, most likely due to the antigens being either dimeric, trimeric
171 or different in size. As we observed differences in responses to sICs vs. immobilized ICs for
172 individual FcγR-ζ reporter cells, this indicates that FcγR ectodomains alone are already able
173 to differentiate between these triggers. To validate this observation in principle, we
174 determined FcγRIIIA activation using primary human NK cells isolated from PBMCs of
175 healthy donors. NK cells were chosen as they mostly express only one type of FcγR similar to
176 our reporter system. Measuring a panel of activation markers and cytokine responses by flow
177 cytometry, we observed a differential activation pattern depending on ICs being soluble or
178 immobilized at equal molarity (Fig. 4A). We chose IL-5/Mpz sICs as NK cells do not express
179 the IL-5 receptor. While MIP1-β responses were comparable between the two triggers,

180 degranulation (CD107a) and TNFα responses showed a trend towards lower activation by
181 sICs compared to immobilized IgG (Mpz). Strikingly, IFNγ responses were significantly
182 weaker when NK cells were incubated with sICs compared to immobilized IgG. In order to
183 confirm this hierarchy of responses and to enhance the overall low activation by Fcγ
184 compared to the PMA control, we changed the IC setup by generating reverse-orientation
185 sICs consisting of human FcγR-specific mouse mAbs and goat-anti-mouse IgG $F(ab)_2$
186 fragments. NK cell activation by reverse sICs was compared to NK cell activation by
187 immobilized FcγR specific mAbs (Fig. 4B). Here, we not only confirm our previous
188 observations regarding MIP-1β and IFNγ, but we also confirm significantly lower TNFα and
189 CD107a responses towards soluble complexes compared to immobilized mAbs. Importantly,
190 these experiments validate that sICs readily activate primary NK cells and induce
191 immunological effector functions. As in roughly 10% of the population NK cells express
192 FcγRIIC (*49-52*), we also tested if this receptor plays a role in our measurements. Using the
193 same three donors and an FcγRII specific mAb as described above, we did not observe an
194 FcγRII-mediated response. Accordingly, we conclude that FcγRIIC expression did not play a
195 role in our experiments (Fig. 4C). Taken together, we show that multivalent but not dimeric
196 soluble immune complexes govern primary NK cell response and FcγRIIIA activation (Fig.
197 2A).
198
199 *Measurement of FcγR activation in response to changing sIC size*
200 We observed that the dimeric sIC CD20:Rtx molecule complex completely failed to trigger
201 FcγRs, while potentially larger sICs based on multimeric antigens showed an efficient dose-
202 dependent FcγR activation. In order to determine whether BW5147 FcγR-ζ reporter cells are
203 able to respond to changes in sIC size, we tested cross-titrated amounts of antibody (mAb,
204 infliximab, Ifx) and antigen (Ag, rhTNFα). To this end, the reporter cells were incubated with
205 sIC of different mAb:Ag ratios by fixing one parameter and titrating the other. According to

206 the Heidelberger-Kendall precipitation curve (*12*) describing sIC size as being dependent on
207 the mAb:Ag ratio, this should result in varying sIC sizes as an excess of either antigen or
208 antibody results in the formation of smaller complexes compared to the large molecular
209 complexes formed at around equal molarity. Changes in sIC size due to a varying mAb:Ag
210 ratio were quantified using asymmetrical flow-field flow fractionation (AF4) (Fig. 5A and
211 Table S1). Fig. S2 shows a complete run of such an analysis. AF4 analysis identifies the
212 highest sIC mean molecular being approximately 2130 kDa at a 1:3 ratio (mAb Ifx : Ag TNF-
213 α) with sICs getting smaller with increasing excess of either antigen or antibody,
214 recapitulating a Heidelberger-Kendall-like curve. Incubation of the FcγR reporter cells with
215 ICs of varying size indeed shows that the assay is sensitive to exactly monitor changes in sIC
216 size (Fig. 5B). Accordingly, both FcγR types showed the strongest responses at mAb:Ag
217 ratios of approximately 1:3. We then set out to test the accuracy of our reporter cell assay as a
218 surrogate for primary human immune cells expressing FcγRs. To this end, we tested primary
219 NK cells from three individual donors and measured NK cell MIP1-β upregulation in
220 response to synthetic sICs of varying size and composition again using a similar assay setup
221 optimized for NK cell activation. We chose MIP-1β upregulation as a cell surface marker to
222 measure NK cell activation as it showed the highest responsiveness in previous experiments
223 (Fig. 4). We could observe that primary immune cells expressing FcγRIIIA respond to IC
224 size, confirming our assay to be an accurate surrogate for primary immune cell responses to
225 soluble ICs (Fig. 5C). Convincingly, NK cell responses to sICs generated from trimeric
226 antigen (rhTNFα) peaked at a different mAb:Ag ratio compared to NK cell responses to sICs
227 generated from dimeric antigens (rhIL-5 and rhVEGFA). Of note, TNFα and VEGFA activate
228 resting NK cells thus leading to higher MIP1-β positivity when NK cells are incubated in the
229 presence of excess antigen. As NK cells do not express IL-5 receptor, this effect is not
230 observed in the presence of excess IL-5. Regarding TNFα, NK cells still show a stronger
231 activation by sICs generated under optimal mAb:Ag ratios compared to conditions where

232 excess antigen is used. The data reveal a direct correlation between sIC size and effector
233 responses. Conversely, when changing antibody concentrations using fixed amounts of
234 antigen, a consistent reduction of NK cell activation is observed in the presence of excess IgG
235 for all three mAb/Ag pairs.
236
237 *Quantification of sIC bioactivity in sera of SLE patients*
238 In order to apply the assay to a clinically relevant condition associated with the occurrence of
239 sICs we measured circulating sICs present in the serum of SLE patients with variable disease
240 activity. Sera from 4 healthy donors and 25 SLE patients were investigated for FcγRIIIA and
241 FcγRIIB/C activation. Reporter cells readily produced IL-2 in response to patient sera in a
242 dose-dependent manner (shown exemplarily for some SLE patients, see Fig. 6A), which was
243 not the case when sera from healthy controls were tested. Consistent with the observation that
244 FcγRI and FcγRIIA do not respond to synthetic sICs, reporter cells expressing these receptors
245 did also not respond to the tested serum samples (Fig. 6A, lower panel). While this reaction
246 pattern already indicated that sICs are the reactive component measured in SLE patients' sera,
247 we further demonstrate that FcγRIIIA and FcγRIIB/C activation depends on the presence of
248 serum ICs by analyzing patient serum before and after polyethylene glycol (PEG)
249 precipitation and depletion of sICs (Fig. 6B). Next, we calculated the area under the curve
250 (AUC) values for all 25 SLE patient titrations and normalized them to the AUC values
251 measured for healthy individuals. The resulting index values were then correlated with
252 established biomarkers of SLE disease activity, such as anti-dsDNA titers (α-dsDNA) and
253 concentrations of the complement cleavage product C3d (Fig. 6C). We observed a significant
254 correlation between our FcγRIIIA activation index values and both of the determined disease
255 activity markers, anti-dsDNA titers and C3d concentration ($p=0.0465$ and $p=0.0052$,
256 respectively). FcγRIIB/C on the other hand showed no significant correlation with either
257 biomarker. We assume these interrelations may be due to the influence of IgG sialyation

258 found to be reduced in active SLE (*53*). Generally, de-sialylation of IgG leads to stronger
259 binding by the activating receptors FcγRI, FcγRIIA and FcγRIII while it reduces the binding
260 affinity of the inhibitory FcγRIIB (*54*). In sum, our assay allows the indirect quantification of
261 clinically relevant sICs in sera of SLE patients.
262
263 *Assay application to clinically relevant in vivo lupus and arthritis mouse models*
264 BW5147 reporter cells stably expressing chimeric mouse as well as rhesus macaque FcγRs
265 have already been generated using the here described methodology and were successfully
266 used to measure FcγR activation by opsonized adherent cells in previous studies (*47, 55*)
267 (mFcγR reporter cells). As the human FcγR reporter cells described here are sensitive to
268 certain sICs, we next aimed to translate the assay to clinically relevant animal models. To this
269 end, we incubated previously described FcγR reporter cells expressing chimeric mouse FcγRs
270 (*47*) with sera from lupus (NZB/WF1) or arthritis (K/BxN) mice with active autoimmune
271 disease. The reporter assay was performed as described above. We chose to measure the
272 stimulation of the activating receptors, mFcγRIII and mFcγRIV, that correspond to human
273 FcγRIII and show a similar cellular distribution and immune function (*16*). Incubation with
274 synthetic sICs generated from rhTNFα and mouse-anti-hTNFα IgG1 showed both of the
275 mFcγR reporter cells to be equally responsive to sICs (Fig. 7A). Parental BW5147 cells
276 expressing no FcγRs served as a control. The sera of three mice per group were analysed and
277 compared to sera from wildtype C57BL/6 mice, which served as a healthy control. C57BL/6
278 mice were chosen, as healthy K/BxN or NZB/WF1 mice cannot be reliably defined. This is
279 due to the unpredictable disease progression in these mouse models starting from a young age.
280 We consistently detected mFcγR activation by sera from K/BxN or NZB/WF1 compared to
281 C57BL6 mice (Fig. 7B). While the mFcγRIII responses were generally high and similar
282 between K/BxN and NZB/WF1 mice, mFcγRIV responsiveness attended to be lower and
283 individually more variable. Altogether, the assay enables the reliable detection of sICs in sera

284 of mice with immune-complex mediated diseases making it a promising novel tool to monitor
285 sICs as a biomarker of disease activity.
286
287 **Discussion**
288 In this study we established, validated and applied a new assay system that is able for the first
289 time to selectively detect soluble multimeric immune complexes as discrete ligands of FcγR.
290 Major findings are i) that sICs cross-link and trigger human FcγRs IIB/C and IIIA but are
291 neglected by activating FcγRI and IIA; ii) that sICs potency is strictly stoichiometry- and size-
292 dependent and thus reproducing the classical Heidelberger-Kendall curve iii) that the overall
293 functional design of FcγRs is adapted to physical cross-linking by soluble vs. membrane-
294 bound immune complexes. The new test system has various obvious applications in medicine
295 and pharmacy.
296
297 *A novel assay for the quantification of disease-associated as well as synthetic sICs*
298 The new approach presents an important and implementable advancement in immunological
299 methodology as it enables the sensitive detection of receptor-activating ICs by a relatively
300 simple, scalable *in vitro* bioassay with high-throughput potential. Based on our pilot study
301 demonstrating that the sIC-mediated FcγRIIIA activation correlated with SLE disease
302 markers, this is of great value for larger prospective clinical studies in patients with
303 autoimmune diseases such as systemic lupus erythematosus (SLE) and rheumatoid arthritis
304 (RA), where circulating ICs have long been shown to crucially contribute to tissue damage
305 and disease manifestations (*40, 41, 56-58*). Disease-associated, endogenous sICs can also
306 occur during infection, e.g. generated after antibody-mediated destruction of pathogenic
307 viruses or microbes or probably more likely due to the oligomeric nature of numerous viral
308 and bacterial structural proteins generated e.g. by SARS-CoV2 (*59-61*) HIV and hepatitis B
309 virus (HBV) infection, during which circulating sICs are generated (*37, 62*). As the assay also

310 enables the sensitive and quantitative measurement of FcγR ligand bioactivity it allows the
311 detection of sICs not only in clinical specimens but also pharmaceutical preparations of IgG
312 and Fc-fusion proteins for therapeutic use (*46*). The presence of ICs in therapeutic
313 preparations or sIC formation following patient treatment is unwanted due to the risk of side
314 effects such as lupus-like syndrome which has been linked to mAb treatment in patients
315 receiving infliximab (*63*) or bevacizumab (*64*), both mAbs used in this study. As this assay is
316 highly sensitive to any aggregation of IgG, it also represents a tool to control the purity,
317 quality and stability of mAb preparations produced for therapeutic use in patients. In addition,
318 the assessment of sIC-mediated FcγR activation allows for optimization of mAbs and Fc-
319 fusion proteins regarding their molecular design and manufacturing. Specifically, Fc-
320 molecules targeting cytokines and soluble factors, which result in sIC formation, could be
321 designed for reduced or enhanced FcγR activation such as glyco-engineered mAbs or LALA-
322 mutant mAbs (*65, 66*). Notably, the scalability of this cell-based test system does allow for
323 large-scale screening of samples.
324
325 *sICs form FcγR ligands with distinct functional profiles*
326 While immobilized ICs decorating infected cells, viral particles or microbial surfaces restrict
327 their triggering effect to a single immune cell residing in very close vicinity, sICs can rapidly
328 disseminate reaching a high number of immune effector cells thus developing a systemic
329 effect with far reaching and long-lasting or even threatening consequences for the host as a
330 whole. This could explain the very tight control of sIC governed effector programs and the
331 unresponsiveness of activating receptors like FcγRI and IIA. We also observed a difference in
332 the response patterns for FcγRIIIA and FcγRII/B/C depending on the solubility of clustered
333 IgG (immobilized versus soluble ICs) which we validated for FcγRIIIA using primary human
334 NK cells (Fig. 4 and 5C). Importantly,only multimeric but not dimeric sICs can trigger FcγR
335 activation. This highlights the fundamental structural influence of the particular antigen as

336 well as the IgG molecule on sIC dimension and subsequent FcγR-mediated signal processing.
337 The ability of the here described assay to define and quantify the activation of individual
338 FcγRs by sIC ligands is not achievable using primary immune cells due to redundant immune
339 responses upon FcγR activation and complex, overlapping expression pattern of FcγRs.
340 Finally, and in contrast to primary human cells, murine BW5147 reporter cells are largely
341 inert to human cytokines, which provides a key advantage to measure FcγR activation
342 selectively in human samples. Notably, the two basically sIC-responsive human FcγR types,
343 i.e. FcγRIIIA and FcγRIIB, are either highly activating versus strongly inhibitory and thus
344 show a mutually exclusive expression pattern (ref. review, z.B. Ravetch und Falk). FcγRIIIA
345 mediates ADCC elicited by NK cells and the induction of a pro-inflammatory cytokine profile
346 by $CD16^{+}$ monocytes, while FcγRIIIB is a GPI-anchored receptor on neutrophils. FcγRIIB is
347 an inhibitory receptor expressed by B cells and dendritic cells (DCs) regulating B cell
348 activation, antibody production by plasma cells and the activation state of DCs, while the
349 activating FcγRIIC is found on NK cells mediating ADCC. However, as FcγRIIC is only
350 expressed by roughly 10% of the human population, its role is still poorly understood (*49-52*).
351 Given the here shown fundamental difference in FcγR reactivity towards multimeric sICs
352 versus immobilized IgG it is tempting to speculate that FcγRIIIA- and FcγRIIB/C-positive
353 immune cells might have evolved to differentially perceive these different FcγR ligands (sICs
354 versus membrane bound insoluble ICs) and translate them into distinct reaction patterns. This
355 could be achieved by differences in receptor density, signal transduction or regulation of
356 receptor expression. Consulting the literature indeed supports our hypothesis with neutrophils,
357 B cells and NK cells being efficiently activated by sICs via almost identical receptor
358 ectodomains (*18, 28, 67, 68*), while the immunological outcome of their triggering very much
359 differs.
360
361

362

363 *Dynamic sIC size measurement and monitoring of bioactivity in sIC-associated diseases*

364 We provide for the first time a simultaneous functional and biophysical assessment of the
365 paradigmatic Heidelberger-Kendall precipitation curve (*12, 13*). While previous work already
366 revealed that large and small sICs differentially impacts IL-6 production in PBMCs (*6*), the
367 dynamics of FcγR activation resulting from constant changes in sIC size have not been
368 explored on a systematic basis. This was undertaken in this study by directly analyzing
369 synthetic ICsformed by highly pure recombinant components via AF4 (Fig. 5A, Fig. S2,
370 Table S1). Our data document that sIC size is indeed governed by antibody:antigen ratios
371 covering a wide range of sizes up to several megadaltons. In the presence of increasing
372 amounts of antibody or antigen deviating from an optimal antibody:ratio, sIC size steadily
373 decreases. Further, by the measurement of FcγR activation we now translate sIC size directly
374 to asimple but precise read-out. In doing so, we show that sIC size essentially tunes FcγR
375 activation on and off. Thus, our new test system can not only contribute to the functional
376 detection and quantification of clinically relevant sICs but also provides a starting point on
377 how to avoid pathological consequences by influencing the sIC size, for example by
378 administering therapeutic antibodies or recombinant antigens in optimized concentrations,
379 thus becoming relevant in clinical pharmacokinetics.

380

381 *Limitations of the reporter system and conclusions*

382 While it is known that FcγRIIA requires FcγRIIIB or FcRn to efficiently respond to ICs (*22,*
383 *23, 69*), unexpectedly, we found that FcγRI is not activated by sICs in our assay. We assume
384 that FcγRI interaction with sICs might require a native cellular environment given that a
385 major function of this FcγR is the uptake and processing of antigen via ICs even in the
386 absence of a signaling motif (*21*). However, we find that FcγRI ectodomains alone are not
387 responsive to sICs implying a thoroughly different cross-linking threshold for FcγRI

388 compared with FcγRIIB and IIIA. This feature is possibly linked to its molecular architecture
389 being the only high-affinity FcγR with three extracellular Ig domains compared to the two
390 domains found in other FcγRs with lower affinity to monomeric IgG. This observation also
391 reflects a general consideration regarding the BW5147 reporter system. While providing a
392 robust and uniform read-out using a scalable cell-based approach, the assay is not able to
393 reflect native immune cell functions governed by cell-intrinsic signalling cascades. The major
394 advancements of this reporter system include i) a higher accuracy regarding FcγR activation
395 compared to merely affinity measurements, ii) an sIC size dependent quantification of FcγR
396 responsiveness and iii) the identification of FcγR activating sICs in autoimmunity and
397 infection. Finally, this scalable, sensitive and robust system to detect FcγR activating sICs in
398 clinical samples might enable their identification in diseases that have not been linked to sIC-
399 mediated pathology, yet.
400
401 **Materials and Methods**
402
403 *Cell culture:* All cells were cultured in a 5% CO_2 atmosphere at 37°C. BW5147 mouse
404 thymoma cells (BW, obtained from ATCC: TIB-47) were maintained at $3x10^5$ to $9x10^5$
405 cells/ml in Roswell Park Memorial Institute medium (RPMI GlutaMAX, Gibco)
406 supplemented with 10% (vol/vol) fetal calf serum (FCS, Biochrom), sodium pyruvate (1x,
407 Gibco) and β-mercaptoethanol (0.1 mM, Gibco). 293T-CD20 (kindly provided by Irvin Chen,
408 UCLA (*70*)) were maintained in Dulbecco's modified Eagle's medium (DMEM, Gibco)
409 supplemented with 10% (vol/vol) FCS.
410
411 *FcγR receptor activation assay:* FcγR activation was measured adapting a previously
412 described cell-based assay (*45, 71*). The assay was modified to measure FcγR activation in
413 solution. Briefly, $2x10^5$ mouse BW-FcγR (BW5147) reporter cells were incubated with

414 synthetic sICs or diluted serum in a total volume of 100 µl for 16 h at 37°C and 5% CO_2.
415 Incubation was performed in a 96-well ELISA plate (Nunc maxisorp) pre-treated with
416 PBS/10% FCS (v/v) for 1 h at 4°C. Immobilized IgG was incubated in PBS on the plates prior
417 to PBS/10% FCS treatment. Reporter cell mIL-2 secretion was quantified via ELISA as
418 described (*45*).
419
420 *Recombinant antigens and monoclonal antibodies to form sICs:* Recombinant human (rh)
421 cytokines TNF, IL-5, and VEGFA were obtained from Stem Cell technologies. Recombinant
422 CD20 was obtained as a peptide (aa141-188) containing the binding region of rituximab
423 (Creative Biolabs). FcγR-specific mAbs were obtained from Stem Cell technologies (CD16:
424 clone 3G8; CD32: IV.3). Reverse sICs were generated from these receptor-specific antibodies
425 using goat-anti-mouse IgG $F(ab)_2$ fragments (Invitrogen) in a 1:1 ratio. Pharmaceutically
426 produced humanized monoclonal IgG1 antibodies infliximab (Ifx), bevacizumab (Bvz),
427 mepolizumab (Mpz) and rituximab (Rtx) were obtained from the University Hospital
428 Pharmacy Freiburg. Mouse anti-hTNFα (IgG2b, R&D Systems, 983003) was used to generate
429 sICs reactive with mouse FcγRs. sICs were generated by incubation of antigens and
430 antibodies in reporter cell medium or PBS for 2 h at 37°C.
431
432 *Lentiviral transduction:* Lentiviral transduction of BW5147 cells was performed as described
433 previously (*47, 55*). In brief, chimeric FcγR-CD3ζ constructs (*45*) were cloned into a
434 pUC2CL6IPwo plasmid backbone. For every construct, one 10-cm dish of packaging cell line
435 at roughly 70% density was transfected with the target construct and two supplementing
436 vectors providing the VSV gag/pol and VSV-G-env proteins (6 µg of DNA each) using
437 polyethylenimine (22.5 µg/ml, Sigma) and Polybrene (4 µg/ml; Merck Millipore) in a total
438 volume of 7 ml (2 ml of a 15-min-preincubated transfection mix in serum-free DMEM added
439 to 5 ml of fresh full DMEM). After a medium change, virus supernatant harvested from the

440 packaging cell line 2 days after transfection was then incubated with target BW cells
441 overnight (3.5 ml of supernatant on 10^6 target cells), followed by expansion and pool
442 selection using complete medium supplemented with 2 µg/ml of puromycin (Sigma) over a
443 one week culture period.
444
445 *BW5147 toxicity test:* Cell counting was performed using a Countess II (Life Technologies)
446 according to supplier instructions. Cell toxicity was measured as a ratio between live and dead
447 cells judged by trypan blue staining over a 16 h time frame in a 96well format (100 µl volume
448 per well). BW5147 cells were mixed 1:1 with Trypan blue (Invitrogen) and analysed using a
449 Countess II. rhTNFα was diluted in complete medium.
450
451 *human IgG suspension ELISA:* 1 µg of IgG1 (rituximab in PBS, 50 µl/well) per well was
452 incubated on a 96well microtiter plate (NUNC Maxisorp) pre-treated (2h at RT) with PBS
453 supplemented with varying percentages (v/v) of FCS (PAN Biotech). IgG1 bound to the
454 plates was detected using an HRP-conjugated mouse-anti-human IgG mAb (Jackson
455 ImmunoResearch).
456
457 *BW5147 cell flow cytometry:* BW5147 cells were harvested by centrifugation at 900 g and RT
458 from the suspension culture. $1x10^6$ cells were stained with PE- or FITC-conjugated anti-
459 human FcγR mAbs (BD) or a PE-TexasRed-conjugated human IgG-Fc fragment (Rockland)
460 for 1h at 4°C in PBS/3%FCS. After 3 washing steps in PBS/3%FCS, the cells were
461 transferred to Flow cytometry tubes (BD) and analysed using BD LSR Fortessa and FlowJo
462 (V10) software.
463
464 *NK cell activation flow cytometry:* PBMC were purified from donor blood using Lymphocyte
465 separation Media (Anprotec). Primary NK cells were separated from donor PBMCs via

466 magnetic bead negative selection (Stem Cell technologies) and NK cell purity was confirmed
467 via staining of CD3 (Biolegend, clone HIT3a), CD16 (Biolegend, clone 3G8) and CD56
468 (Miltenyi Biotec, clone AF12-7H3). 96well ELISA plates (Nunc Maxisorp) were pre-treated
469 with PBS/10% FCS (v/v) for 1 h at 4°C. NK cells were stimulated in pre-treated plates and
470 incubated at 37°C and 5% CO_2 for 4 h. Golgi Plug and Golgi Stop solutions (BD) were added
471 as suggested by supplier. CD107a (APC, BD, H4A3) specific conjugated mAb was added at
472 the beginning of the incubation period. Following the stimulation period, MIP-1β (PE, BD
473 Pharmigen), IFNγ (BV-510, Biolegends, 4SB3) and TNFα (PE/Cy7, Biolegends, MAB11)
474 production was measured via intracellular staining Cytokines (BD, CytoFix/CytoPerm, Kit as
475 suggested by the supplier). 50 ng/ml PMA (InvivoGen) + 0.5 µM Ionomycin (InvivoGen)
476 were used as a positive stimulation control for NK cell activation. After 3 washing steps in
477 PBS/3%FCS, the cells were transferred to Flow cytometry tubes (BD) and analysed using a
478 BD FACS Fortessa and FlowJo (V10) software. FcγRII or FcγRIII block was performed by
479 addition of receptor specific mAbs (Stem cell technologies, IV.3 and 3G8) at a 1:100 dilution
480 at the beginning of the incubation period. Cells were transferred to Flow cytometry tubes
481 (BD) and analyzed using BD LSR Fortessa and FlowJo (V10) software.
482
483 *Asymmetric flow field flow fractionation (AF4):* The AF4 system consisted of a flow
484 controller (Eclipse AF4, Wyatt), a MALS detector (DAWN Heleos II, Wyatt), a UV detector
485 (1260 Infinity G1314F, Agilent) and the separation channel (SC channel, PES membrane, cut-
486 off 10 kDa, 490 µm spacer, wide type, Wyatt). Elution buffer: 1.15 g/L Na_2HPO_4 (Merck),
487 0.20 g/L NaH_2PO_4 x H_2O (Merck), 8.00 g/L NaCl (Sigma) and 0,20 g/L NaN_3 (Sigma),
488 adjusted to pH 7.4, filtered through 0.1 µm. AF4 sequence (Vx = cross flow in mL/min): (a)
489 elution (2 min, Vx: 1.0); (b) focus (1 min, Vx: 1.0), focus + inject (1 min, Vx: 1.0, inject flow:
490 0.2 mL/min), repeated three times; (c) elution (30 min, linear Vx gradient: 1.0 to 0.0); (d)
491 elution (15 min, Vx: 0.0); (e) elution + inject (5 min, Vx: 0.0). A total protein mass of 17±0.3

492 μg (Ifx, rhTNFα or ICs, respectively) was injected. The eluted sample concentration was
493 calculated from the UV signal at 280 nm using extinction coefficients of 1.240 mL/(mg cm)
494 or 1.450 mL/(mg cm) in the case of TNFα or Ifx, respectively. For the ICs, extinction
495 coefficients were not available and difficult to calculate as the exact stoichiometry is not
496 known. An extinction coefficient of 1.450 mL/(mg cm) was used for calculating the molar
497 masses of all ICs. Especially in the case of ICs rich in TNFα, the true coefficients should be
498 lower, and the molar masses of these complexes are overestimated by not more than 14 %.
499 The determined molar masses for TNFα-rich complexes are therefore biased but the observed
500 variations in molar mass for the different ICs remain valid. The mass-weighted mean of the
501 distribution of molar masses for each sample was calculated using the ASTRA 7 software
502 package (Wyatt).
503
504 *SLE patient cohort:* Sera from patients with SLE were obtained from the Immunologic,
505 Rheumatologic Biobank (IR-B) of the Department of Rheumatology and Clinical
506 Immunology. Biobanking and the project were approved by the local ethical committee of the
507 University of Freiburg (votes 507/16 and 624/14). All patients who provided blood to the
508 biobank had provided written informed consent. Ethical Statement: The study was designed in
509 accordance with the guidelines of the Declaration of Helsinki (revised 2013). Patients with
510 SLE (n = 25) and healthy controls (n = 4) were examined. All patients met the revised ACR
511 classification criteria for SLE. Disease activity was assessed using the SLEDAI-2K score.
512 C3d levels were analyzed in EDTA plasma using rocket double decker immune-
513 electrophoresis with antisera against C3d (Polyclonal Rabbit Anti-Human C3d Complement,
514 Agilent) and C3c (Polyclonal Rabbit Anti-Human C3c Complement Agilent) as previously
515 described (*72*). Anti-human dsDNA antibodies titers were determined in serum using an anti-
516 dsDNA IgG ELISA kit (diagnostik-a GmbH).
517

518 *Patient serum IC precipitation:* For polyethylene glycol (PEG) precipitation human sera were
519 mixed with PEG 6000 (Sigma-Aldrich) in PBS at a final concentration of 10% PEG 6000.
520 After overnight incubation at 4°C, ICs were precipitated by centrifugation at 2000 x g for
521 30 min at 4 °C, pellets were washed once with PEG 6000 and then centrifugated at 2000 x g
522 for 20 min at 4 °C. Supernatants were harvested and precipitates re-suspended in pre-warmed
523 PBS for 1 h at 37 °C. IgG concentrations of serum, precipitates and supernatants obtained
524 after precipitation were quantified by Nanodrop (Thermo Scientific™) measurement.
525
526 *Mice and Models:* Animal experiments were approved by the local governmental commission
527 for animal protection of Freiburg (Regierungspräsidium Freiburg, approval no. G16/59 and
528 G19/21). Lupus-prone (NZBxNZW)F1 mice (NZB/WF1) were generated by crossing
529 NZB/BlNJ mice with NZW/LacJ mice, purchased from The Jackson Laboratory. KRNtg mice
530 were obtained from F. Nimmerjahn (Universität Erlangen-Nürnberg) with the permission of
531 D. Mathis and C. Benoist (Harvard Medical School, Boston, MA), C57BL/6 mice (BL/6) and
532 NOD/ShiLtJArc (NOD/Lt) mice were obtained from the Charles River Laboratories. K/BxN
533 (KRNtgxNOD)F1 mice (K/BxN) were obtained by crossing KRNtg mice and NOD/Lt mice.
534 All mice were housed in a 12-h light/dark cycle, with food and water ad libitum. Mice were
535 euthanized and blood collected for serum preparation from 16 weeks old BL/6 animals, from
536 16 weeks old arthritic K/BxN animals and from 26 – 38 weeks old NZB/WF1 mice with
537 established glomerulonephritis.
538
539 *Statistical analyses:* Statistical analyses were performed using Graphpad Prism software (v6)
540 and appropriate tests.
541
542
543

Acknowledgements: We thank T. Schleyer (IR-B Biobank) for providing patient samples. We are indebted to Falk. Nimmerjahn (Universität Erlangen-Nürnberg) for providing KRNtg mice. **Funding:** This work was supported by an intramural junior investigator fund of the Faculty of Medicine to PK (EQUIP - Funding for Medical Scientists, Faculty of Medicine, University of Freiburg), by the German Research foundation (DFG) (FOR2830 HE 2526/9-1) and NaFoUniMedCovid19“ (FKZ: 01KX2021) – COVIM and FKZ 100493916 B-FAST to HH, by the DFG research grant TRR130 to REV and the Ministry of Science, Research, and Arts Baden-Württemberg (Margarete von Wrangell Programm) to NC. **Author contributions:** HC and PK designed and developed the reporter system, conducted Fc-gamma receptor activation experiments and prepared synthetic immune complexes. AMP, US and REV manage the SLE patient cohort, provided sera and performed immune complex precipitation as well as IgG quantification. MH designed and performed AF4 analyses. NC manages the mouse models and provided sera. HH and PK supervised all experiments. HC and PK analysed and interpreted data. PK wrote the paper assisted by HC, AMP, MH, NC, REV and HH. **Competing interests:** The authors declare no financial and non-financial competing interests. **Data and materials availability:** All data associated with this study are present in the paper or Supplementary Materials.

Supplementary Materials

Fig. S1. rhTNFα is not toxic to mouse lymphocyte BW5147 cells even at high concentrations.

Fig. S2. AF4 elution profiles of Ifx/TNFα-immune complexes.

Table S1. Analysis of the molar mass distribution of ICs from AF4 data.

568 **References**

569 1. L. L. Lu, T. J. Suscovich, S. M. Fortune, G. Alter, Beyond binding: antibody effector
570 functions in infectious diseases. *Nat Rev Immunol* **18**, 46-61 (2018).
571 2. J. V. Ravetch, S. Bolland, IgG Fc receptors. *Annu Rev Immunol* **19**, 275-290 (2001).
572 3. C. E. van der Poel, R. M. Spaapen, J. G. van de Winkel, J. H. Leusen, Functional
573 characteristics of the high affinity IgG receptor, FcgammaRI. *J Immunol* **186**, 2699-
574 2704 (2011).
575 4. P. Bruhns *et al.*, Specificity and affinity of human Fcgamma receptors and their
576 polymorphic variants for human IgG subclasses. *Blood* **113**, 3716-3725 (2009).
577 5. D. Urlaub *et al.*, Activation of natural killer cells by rituximab in granulomatosis with
578 polyangiitis. *Arthritis Res Ther* **21**, 277 (2019).
579 6. A. Lux, X. Yu, C. N. Scanlan, F. Nimmerjahn, Impact of immune complex size and
580 glycosylation on IgG binding to human FcgammaRs. *J Immunol* **190**, 4315-4323
581 (2013).
582 7. F. Kiefer *et al.*, The Syk protein tyrosine kinase is essential for Fc gamma receptor
583 signaling in macrophages and neutrophils. *Mol Cell Biol* **18**, 4209-4220 (1998).
584 8. Y. Luo, J. W. Pollard, A. Casadevall, Fcgamma receptor cross-linking stimulates cell
585 proliferation of macrophages via the ERK pathway. *J Biol Chem* **285**, 4232-4242
586 (2010).
587 9. S. Greenberg, P. Chang, S. C. Silverstein, Tyrosine phosphorylation of the gamma
588 subunit of Fc gamma receptors, p72syk, and paxillin during Fc receptor-mediated
589 phagocytosis in macrophages. *J Biol Chem* **269**, 3897-3902 (1994).
590 10. S. Bournazos, T. T. Wang, R. Dahan, J. Maamary, J. V. Ravetch, Signaling by
591 Antibodies: Recent Progress. *Annu Rev Immunol* **35**, 285-311 (2017).
592 11. F. Nimmerjahn, J. V. Ravetch, Antibody-mediated modulation of immune responses.
593 *Immunol Rev* **236**, 265-275 (2010).
594 12. M. Heidelberger, F. E. Kendall, A Quantitative Study of the Precipitin Reaction
595 between Type Iii Pneumococcus Polysaccharide and Purified Homologous Antibody.
596 *J Exp Med* **50**, 809-823 (1929).
597 13. M. Heidelberger, F. E. Kendall, The Precipitin Reaction between Type Iii
598 Pneumococcus Polysaccharide and Homologous Antibody : Iii. A Quantitative Study
599 and a Theory of the Reaction Mechanism. *J Exp Med* **61**, 563-591 (1935).
600 14. A. M. Duchemin, L. K. Ernst, C. L. Anderson, Clustering of the High-Affinity Fc
601 Receptor for Immunoglobulin-G (Fc-Gamma-Ri) Results in Phosphorylation of Its
602 Associated Gamma-Chain. *J Biol Chem* **269**, 12111-12117 (1994).
603 15. A. Getahun, J. C. Cambier, Of ITIMs, ITAMs, and ITAMis: revisiting immunoglobulin
604 Fc receptor signaling. *Immunol Rev* **268**, 66-73 (2015).
605 16. P. Bruhns, F. Jonsson, Mouse and human FcR effector functions. *Immunol Rev* **268**,
606 25-51 (2015).
607 17. P. Bruhns, Properties of mouse and human IgG receptors and their contribution to
608 disease models. *Blood* **119**, 5640-5649 (2012).
609 18. F. Nimmerjahn, J. V. Ravetch, Fcgamma receptors as regulators of immune
610 responses. *Nat Rev Immunol* **8**, 34-47 (2008).
611 19. F. Nimmerjahn, J. V. Ravetch, Fcgamma receptors: old friends and new family
612 members. *Immunity* **24**, 19-28 (2006).
613 20. M. Guilliams, P. Bruhns, Y. Saeys, H. Hammad, B. N. Lambrecht, The function of
614 Fcgamma receptors in dendritic cells and macrophages. *Nat Rev Immunol* **14**, 94-108
615 (2014).
616 21. Z. K. Indik *et al.*, The high affinity Fc gamma receptor (CD64) induces phagocytosis in
617 the absence of its cytoplasmic domain: the gamma subunit of Fc gamma RIIIA
618 imparts phagocytic function to Fc gamma RI. *Exp Hematol* **22**, 599-606 (1994).
619 22. G. Fossati, R. C. Bucknall, S. W. Edwards, Insoluble and soluble immune complexes
620 activate neutrophils by distinct activation mechanisms: changes in functional
621 responses induced by priming with cytokines. *Ann Rheum Dis* **61**, 13-19 (2002).

622 23. J. J. Hubbard *et al.*, FcRn is a CD32a coreceptor that determines susceptibility to IgG
623 immune complex-driven autoimmunity. *J Exp Med* **217**, (2020).
624 24. A. Pincetic *et al.*, Type I and type II Fc receptors regulate innate and adaptive
625 immunity. *Nat Immunol* **15**, 707-716 (2014).
626 25. G. Vidarsson, G. Dekkers, T. Rispens, IgG subclasses and allotypes: from structure
627 to effector functions. *Front Immunol* **5**, 520 (2014).
628 26. M. Z. Tay, K. Wiehe, J. Pollara, Antibody-Dependent Cellular Phagocytosis in
629 Antiviral Immune Responses. *Front Immunol* **10**, 332 (2019).
630 27. E. A. Laborde *et al.*, Immune complexes inhibit differentiation, maturation, and
631 function of human monocyte-derived dendritic cells. *J Immunol* **179**, 673-681 (2007).
632 28. S. Kang *et al.*, IgG-Immune Complexes Promote B Cell Memory by Inducing BAFF. *J*
633 *Immunol* **196**, 196-206 (2016).
634 29. V. Granger, M. Peyneau, S. Chollet-Martin, L. de Chaisemartin, Neutrophil
635 Extracellular Traps in Autoimmunity and Allergy: Immune Complexes at Work. *Front*
636 *Immunol* **10**, 2824 (2019).
637 30. S. Berger, H. Ballo, H. J. Stutte, Immune complex-induced interleukin-6, interleukin-
638 10 and prostaglandin secretion by human monocytes: A network of pro- and anti-
639 inflammatory cytokines dependent on the antigen:antibody ratio. *Eur J Immunol* **26**,
640 1297-1301 (1996).
641 31. L. Koenderman, Inside-Out Control of Fc-Receptors. *Front Immunol* **10**, 544 (2019).
642 32. R. Plomp *et al.*, Subclass-specific IgG glycosylation is associated with markers of
643 inflammation and metabolic health. *Sci Rep* **7**, 12325 (2017).
644 33. T. C. Pierson *et al.*, The stoichiometry of antibody-mediated neutralization and
645 enhancement of West Nile virus infection. *Cell Host Microbe* **1**, 135-145 (2007).
646 34. K. R. Patel, J. T. Roberts, A. W. Barb, Multiple Variables at the Leukocyte Cell
647 Surface Impact Fc gamma Receptor-Dependent Mechanisms. *Front Immunol* **10**, 223
648 (2019).
649 35. S. Bohm, D. Kao, F. Nimmerjahn, Sweet and sour: the role of glycosylation for the
650 anti-inflammatory activity of immunoglobulin G. *Current topics in microbiology and*
651 *immunology* **382**, 393-417 (2014).
652 36. R. J. Stopforth *et al.*, Detection of Experimental and Clinical Immune Complexes by
653 Measuring SHIP-1 Recruitment to the Inhibitory FcgammaRIIB. *J Immunol* **200**, 1937-
654 1950 (2018).
655 37. T. T. Wang, J. V. Ravetch, Immune complexes: not just an innocent bystander in
656 chronic viral infection. *Immunity* **42**, 213-215 (2015).
657 38. D. H. Yamada *et al.*, Suppression of Fcgamma-receptor-mediated antibody effector
658 function during persistent viral infection. *Immunity* **42**, 379-390 (2015).
659 39. U. Antes, H. P. Heinz, D. Schultz, D. Brackertz, M. Loos, C1q-bearing immune
660 complexes detected by a monoclonal antibody to human C1q in rheumatoid arthritis
661 sera and synovial fluids. *Rheumatol Int* **10**, 245-250 (1991).
662 40. R. H. Zubler *et al.*, Circulating and intra-articular immune complexes in patients with
663 rheumatoid arthritis. Correlation of 125I-Clq binding activity with clinical and biological
664 features of the disease. *J Clin Invest* **57**, 1308-1319 (1976).
665 41. D. Koffler, V. Agnello, R. Thoburn, H. G. Kunkel, Systemic lupus erythematosus:
666 prototype of immune complex nephritis in man. *J Exp Med* **134**, 169-179 (1971).
667 42. T. V. Rajan, The Gell-Coombs classification of hypersensitivity reactions: a re-
668 interpretation. *Trends in immunology* **24**, 376-379 (2003).
669 43. S. Tahir *et al.*, A CD153+CD4+ T follicular cell population with cell-senescence
670 features plays a crucial role in lupus pathogenesis via osteopontin production. *J*
671 *Immunol* **194**, 5725-5735 (2015).
672 44. A. Bano *et al.*, CD28 (null) CD4 T-cell expansions in autoimmune disease suggest a
673 link with cytomegalovirus infection. *F1000Res* **8**, (2019).
674 45. E. Corrales-Aguilar *et al.*, A novel assay for detecting virus-specific antibodies
675 triggering activation of Fcgamma receptors. *Journal of immunological methods* **387**,
676 21-35 (2013).

677 46. H. A. D. Lagasse, H. Hengel, B. Golding, Z. E. Sauna, Fc-Fusion Drugs Have
678 FcgammaR/C1q Binding and Signaling Properties That May Affect Their
679 Immunogenicity. *AAPS J* **21**, 62 (2019).
680 47. S. Van den Hoecke *et al.*, Hierarchical and Redundant Roles of Activating
681 FcgammaRs in Protection against Influenza Disease by M2e-Specific IgG1 and
682 IgG2a Antibodies. *J Virol* **91**, (2017).
683 48. M. Tanaka *et al.*, Activation of Fc gamma RI on monocytes triggers differentiation into
684 immature dendritic cells that induce autoreactive T cell responses. *J Immunol* **183**,
685 2349-2355 (2009).
686 49. S. Lisi, M. Sisto, D. D. Lofrumento, S. D'Amore, M. D'Amore, Advances in the
687 understanding of the Fc gamma receptors-mediated autoantibodies uptake. *Clin Exp*
688 *Med* **11**, 1-10 (2011).
689 50. J. C. Anania, A. M. Chenoweth, B. D. Wines, P. M. Hogarth, The Human
690 FcgammaRII (CD32) Family of Leukocyte FcR in Health and Disease. *Front Immunol*
691 **10**, 464 (2019).
692 51. D. Metes *et al.*, Expression of functional CD32 molecules on human NK cells is
693 determined by an allelic polymorphism of the FcgammaRIIC gene. *Blood* **91**, 2369-
694 2380 (1998).
695 52. W. B. Breunis *et al.*, Copy number variation of the activating FCGR2C gene
696 predisposes to idiopathic thrombocytopenic purpura. *Blood* **111**, 1029-1038 (2008).
697 53. F. Vuckovic *et al.*, Association of systemic lupus erythematosus with decreased
698 immunosuppressive potential of the IgG glycome. *Arthritis Rheumatol* **67**, 2978-2989
699 (2015).
700 54. Y. Kaneko, F. Nimmerjahn, J. V. Ravetch, Anti-inflammatory activity of
701 immunoglobulin G resulting from Fc sialylation. *Science* **313**, 670-673 (2006).
702 55. P. Kolb *et al.*, Identification and Functional Characterization of a Novel Fc Gamma-
703 Binding Glycoprotein in Rhesus Cytomegalovirus. *J Virol* **93**, (2019).
704 56. U. E. Nydegger, J. S. t. Davis, Soluble immune complexes in human disease. *CRC*
705 *Crit Rev Clin Lab Sci* **12**, 123-170 (1980).
706 57. R. J. Levinsky, J. S. Cameron, J. F. Soothill, Serum immune complexes and disease
707 activity in lupus nephritis. *Lancet* **1**, 564-567 (1977).
708 58. R. J. Levinsky, Role of circulating soluble immune complexes in disease. *Arch Dis*
709 *Child* **53**, 96-99 (1978).
710 59. L. Briant, N. Coudronniere, V. Robert-Hebmann, M. Benkirane, C. Devaux, Binding of
711 HIV-1 virions or gp120-anti-gp120 immune complexes to HIV-1-infected quiescent
712 peripheral blood mononuclear cells reveals latent infection. *J Immunol* **156**, 3994-
713 4004 (1996).
714 60. S. K. Oh *et al.*, Identification of HIV-1 envelope glycoprotein in the serum of AIDS and
715 ARC patients. *J Acquir Immune Defic Syndr (1988)* **5**, 251-256 (1992).
716 61. D. A. Vuitton, L. Vuitton, E. Seilles, P. Galanaud, A plea for the pathogenic role of
717 immune complexes in severe Covid-19. *Clin Immunol* **217**, 108493 (2020).
718 62. K. Madalinski, B. Burczynska, K. H. Heermann, A. Uy, W. H. Gerlich, Analysis of viral
719 proteins in circulating immune complexes from chronic carriers of hepatitis B virus.
720 *Clin Exp Immunol* **84**, 493-500 (1991).
721 63. D. A. Wetter, M. D. Davis, Lupus-like syndrome attributable to anti-tumor necrosis
722 factor alpha therapy in 14 patients during an 8-year period at Mayo Clinic. *Mayo Clin*
723 *Proc* **84**, 979-984 (2009).
724 64. D. A. MacDonald *et al.*, Aflibercept exhibits VEGF binding stoichiometry distinct from
725 bevacizumab and does not support formation of immune-like complexes.
726 *Angiogenesis* **19**, 389-406 (2016).
727 65. K. O. Saunders, Conceptual Approaches to Modulating Antibody Effector Functions
728 and Circulation Half-Life. *Front Immunol* **10**, 1296 (2019).
729 66. T. Li *et al.*, Modulating IgG effector function by Fc glycan engineering. *Proceedings of*
730 *the National Academy of Sciences of the United States of America* **114**, 3485-3490
731 (2017).

732 67. M. R. Goodier *et al.*, Sustained Immune Complex-Mediated Reduction in CD16
733 Expression after Vaccination Regulates NK Cell Function. *Front Immunol* **7**, 384
734 (2016).
735 68. T. N. Mayadas, G. C. Tsokos, N. Tsuboi, Mechanisms of immune complex-mediated
736 neutrophil recruitment and tissue injury. *Circulation* **120**, 2012-2024 (2009).
737 69. S. Nagarajan *et al.*, Cell-specific, activation-dependent regulation of neutrophil
738 CD32A ligand-binding function. *Blood* **95**, 1069-1077 (2000).
739 70. K. Morizono *et al.*, Redirecting lentiviral vectors pseudotyped with Sindbis virus-
740 derived envelope proteins to DC-SIGN by modification of N-linked glycans of
741 envelope proteins. *J Virol* **84**, 6923-6934 (2010).
742 71. E. Corrales-Aguilar *et al.*, Human cytomegalovirus Fcgamma binding proteins gp34
743 and gp68 antagonize Fcgamma receptors I, II and III. *PLoS pathogens* **10**, e1004131
744 (2014).
745 72. E. Rother, B. Lang, R. Coldewey, K. Hartung, H. H. Peter, Complement split product
746 C3d as an indicator of disease activity in systemic lupus erythematosus. *Clin*
747 *Rheumatol* **12**, 31-35 (1993).

748

749

750 **Figures**

751

752 **Figure 1**

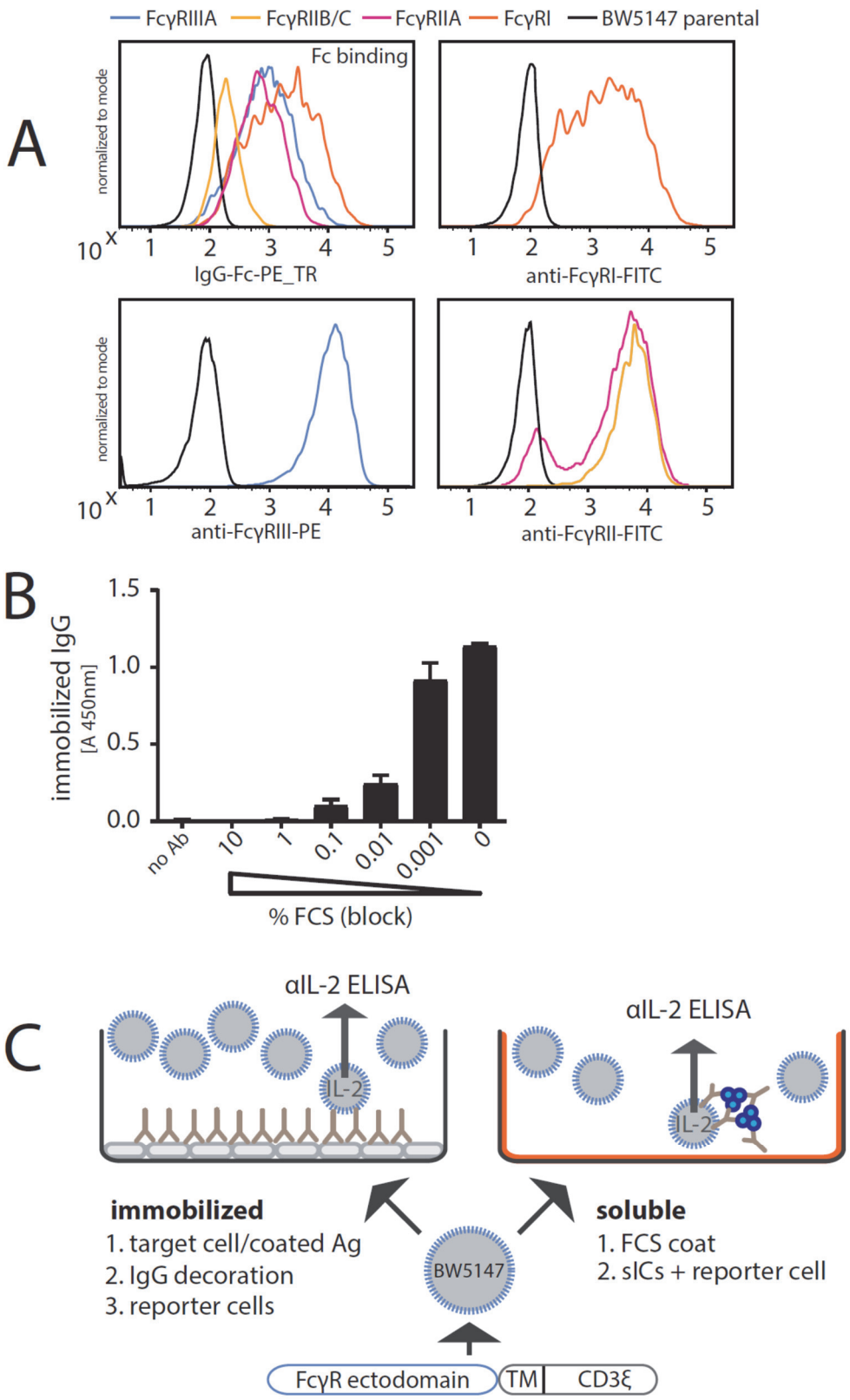

753

754

755 **Figure 2**

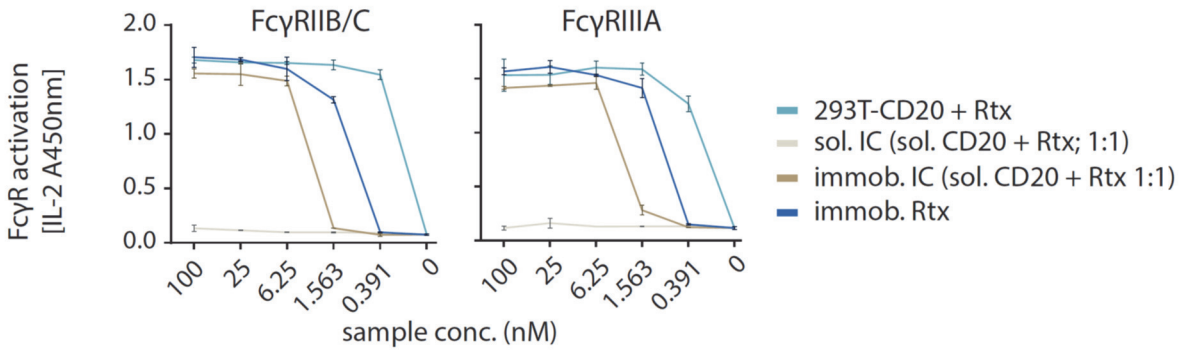

756

757 **Fig. 2. FcγRIIB/C and FcγRIIIA do not respond to small hetero-dimeric sICs but are**
758 **sensitive to immobilized IgG/ICs.** Dose-dependent activation of FcγR-bearing reporter cells
759 by immobilized IC can be mimicked by immobilized IgG. Response curves of human
760 FcγRIIB/C and FcγRIIIA are similar between opsonized cells (293T cells stably expressing
761 CD20 + Rtx), immobilized IC (rec. soluble CD20 + Rtx) and immobilized IgG (Rtx). sIC
762 formed by monovalent antigen (rec. soluble CD20) do not activate human FcγRs. X-Axis
763 shows sample concentration determined by antibody molarity. Y-Axis shows FcγR activation
764 determined by reporter cell IL-2 production.

765

766 **Figure 3**

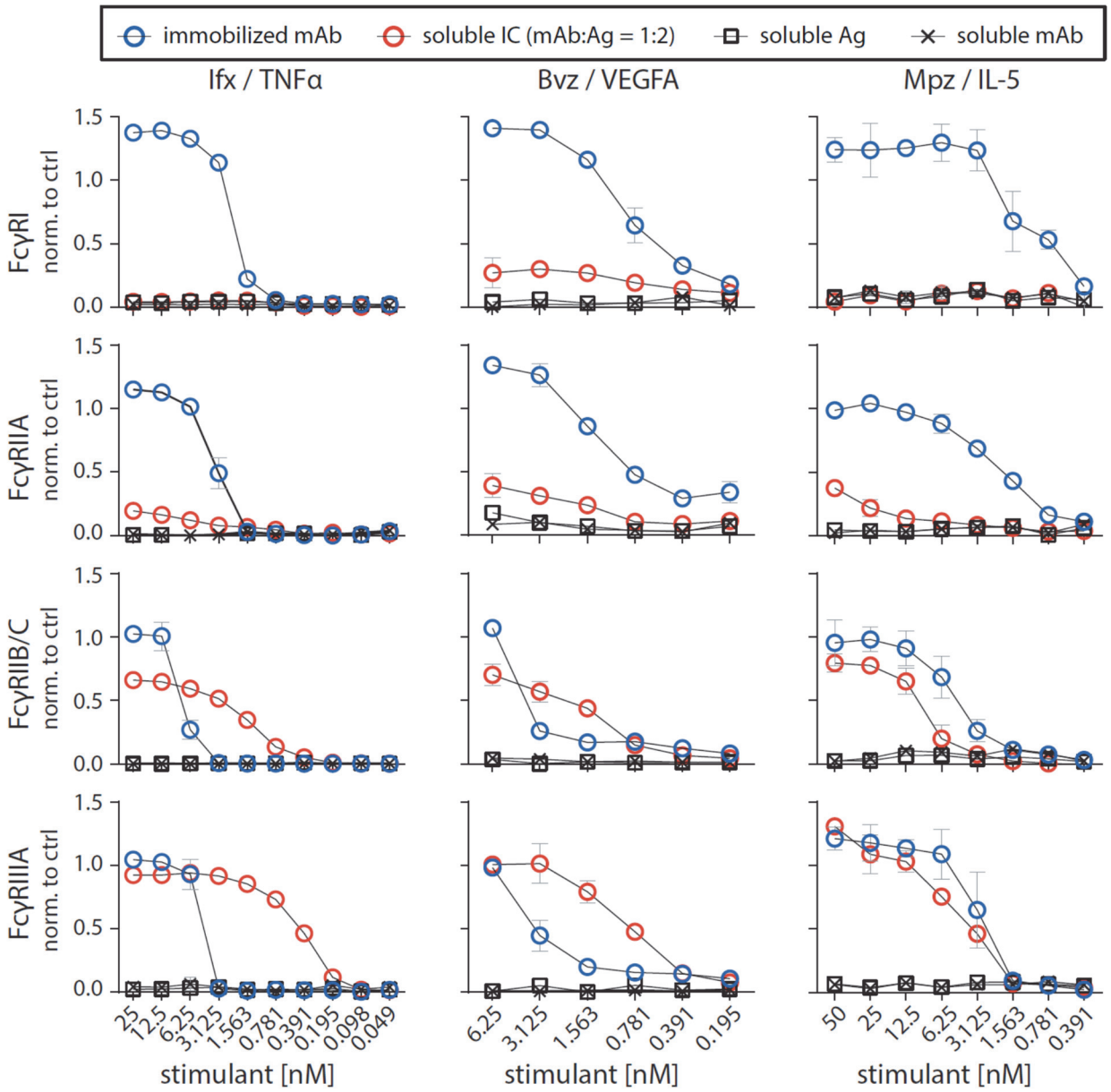

767
768

769 **Fig. 3. FcγRIIB/C and FcγRIIIA are activated by sICs formed from multivalent**
770 **antigens.** Three different multivalent ultra-pure antigens (Ag) mixed with respective therapy-
771 grade mAbs were used to generate sICs as indicated for each set of graphs (top to bottom). IC
772 pairs: infliximab (Ifx) and rhTNFα; mepolizumab (Mpz) and rhIL-5; bevacizumab (Bvz) and
773 rhVEGFA. X-Axis: concentrations of stimulant expressed as molarity of either mAb or Ag
774 monomer and IC (expressed as mAb molarity) at a mAb:Ag ratio of 1:2. Soluble antigen or
775 soluble antibody alone served as negative controls and were not sufficient to activate human
776 FcγRs. FcγR responses were normalized to immobilized rituximab (Rtx) at 1μg/well (set to 1)
777 and a medium control (set to 0). All FcγRs show dose-dependent activation towards
778 immobilized IgG. FcγRIIA shows low activation at high sIC concentrations compared to
779 immobilized IgG activation. FcγRI shows no activation towards sICs. FcγRIIIA and
780 FcγRIIB/C are dose-dependently activated by sICs with responses comparable in strength to
781 immobilized IgG stimulant. Experiments performed in technical replicates. Error bars = SD.
782 Error bars smaller than symbols are not shown.

783 **Figure 4**

784

785

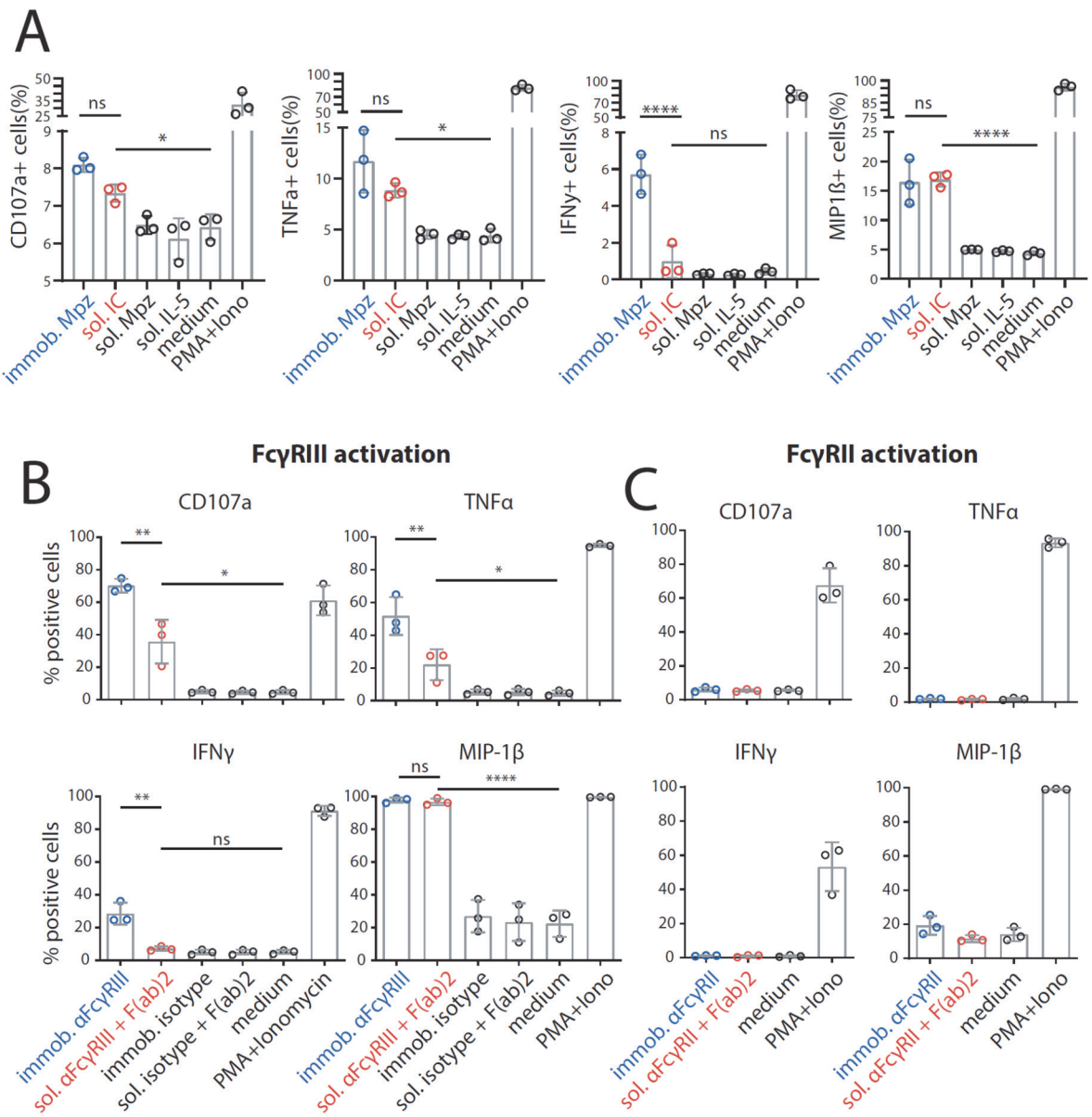

786

787

788

789 **Fig. 4. The FcγRIII-dependent activation pattern of primary NK cells depends on IC**
790 **solubility**. Negatively selected primary NK cells purified from PBMCs of three healthy
791 donors were tested for NK cell activation markers. Error bars = SD. Two-way ANOVA
792 (Turkey). A) NK cells were incubated with immobilized IgG (mepolizumab, Mpz), soluble IC
793 (Mpz:IL-5 = 1:1), soluble Mpz or soluble IL-5 (all at 200 nM, 10^6 cells). Incubation with
794 PMA and Ionomycin (Iono) served as a positive control. Incubation with medium alone
795 served as a negative control. B) NK cells were incubated for 4 h with immobilized FcγRIII-
796 specific mAb, soluble mouse-anti-human IgG $F(ab)_2$ complexed FcγRIII-specific mAb
797 (reverse sICs), immobilized IgG of non-FcγRIII-specificity (isotype control) or soluble $F(ab)_2$
798 complexed isotype control (all at 1µg, 10^6 cells). Incubation with PMA and Ionomycin served
799 as a positive control. Incubation with medium alone served as a negative control. C) As in B
800 using an FcγRII-specific mAb. NK cells from the tested donors in this study do not react to
801 FcγRII activation.

802 **Figure 5**

803

804

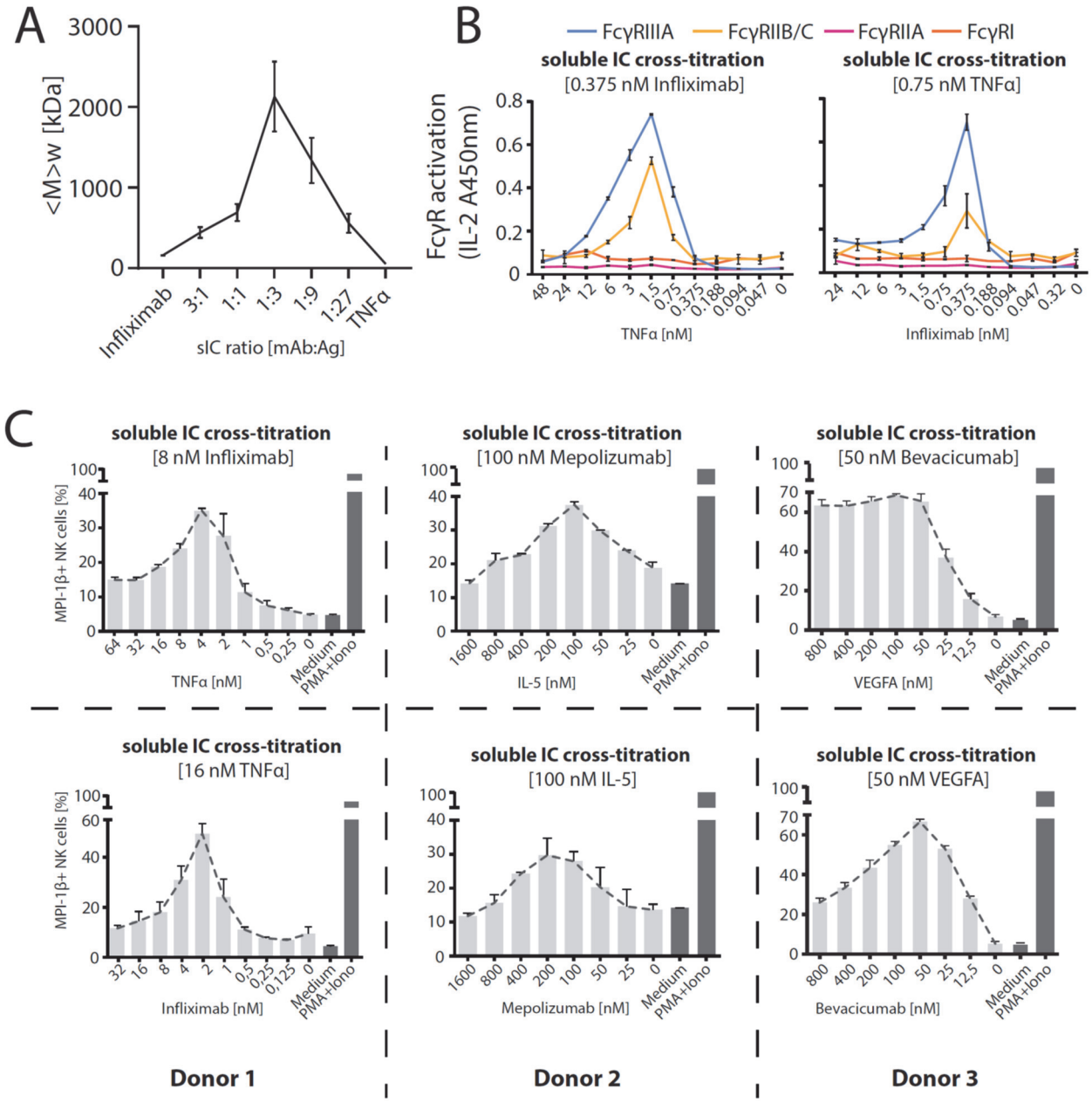

805

806

807 **Fig. 5. FcγRIIB/C and FcγR-IIIA respond to sIC size reproducing a Heidelberger-**
808 **Kendall like precipitation curve.** A) infliximab (mAb) and rhTNFα (Ag) were mixed at
809 different ratios (17 µg total protein, calculated from monomer molarity) and analysed via
810 AF4. sIC size is maximal at a 1:3 ratio of mAb:Ag and reduced when either mAb or Ag are
811 given in excess. $\langle M \rangle_w$ = mass-weighted mean of the molar mass distribution. Three
812 independent experiments. Error bars = SD. Data taken from Table S1. One complete run
813 analysis is shown in Fig. S2. B) FcγR BW5147 reporter cell activation is sensitive to sIC size.
814 sICs of different size were generated by cross-titration according to the AF4 determination.
815 Reporter cells were incubated with fixed amounts of either mAb (infliximab, left) or Ag
816 (rhTNFα, right) and titrated amounts of antigen or antibody, respectively. X-Axis shows
817 titration of either antigen or antibody, respectively (TNFα calculated as monomer). IL-2
818 production of reporter cells shows a peak for FcγRIIB/C and FcγRIIIA activation at an
819 antibody:antigen ratio between 1:2 and 1:4. FcγRs I and IIA show no activation towards sICs
820 in line with previous observations, see Fig.3. Two independent experiments. Error bars = SD.
821 C) Purified primary NK cells from three different donors were incubated with cross-titrated
822 sICs as in A. NK cells were measured for MIP-1β expression (% positivity). Incubation with
823 PMA and Ionomycin served as a positive control. Incubation with medium alone served as a
824 negative control. Measured in technical replicates. Error bars = SD.

825 **Figure 6**

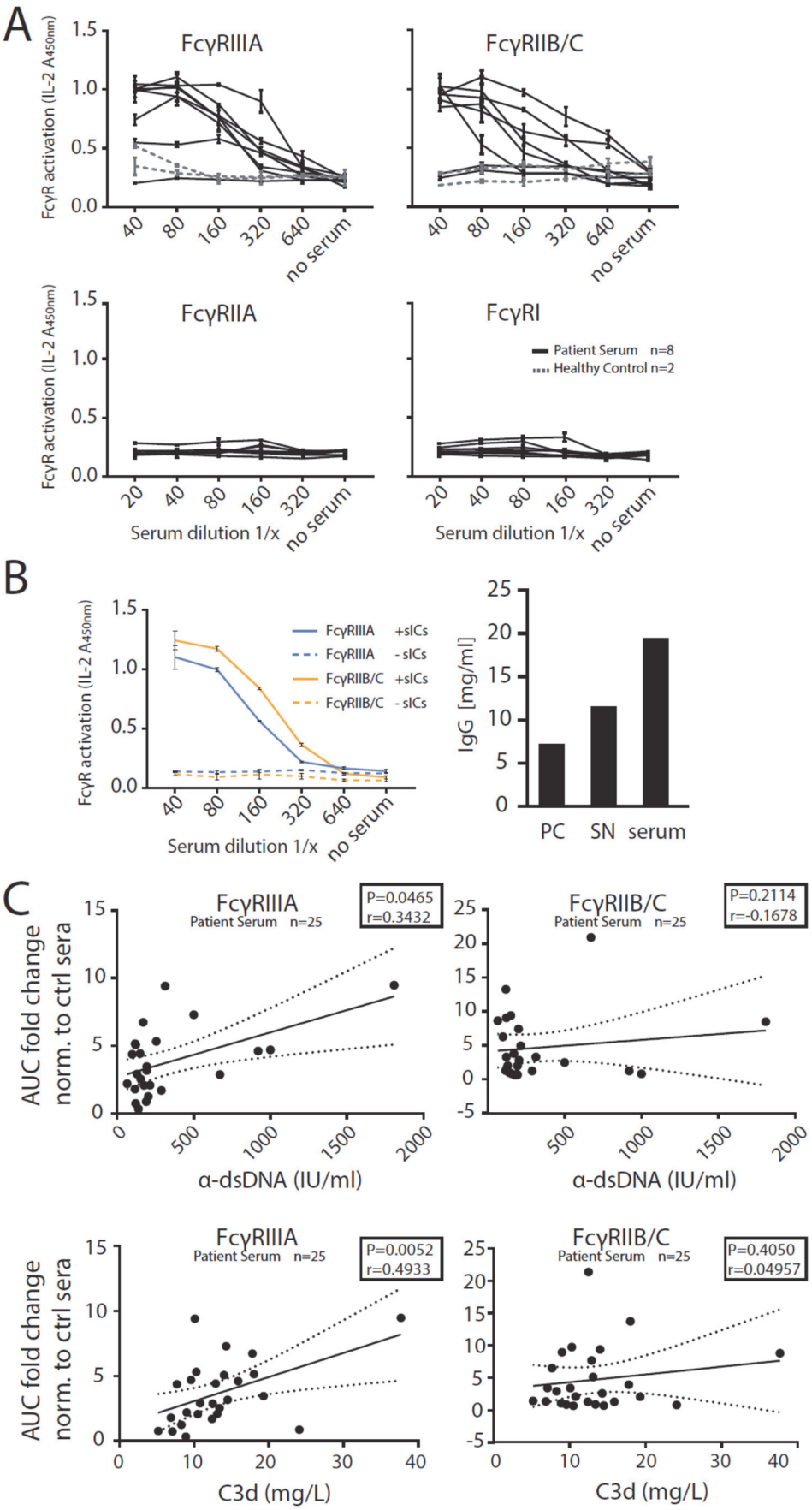

826

827 **Fig. 6. The reporter assay enables quantification of serum-derived sICs from SLE**
828 **patients.** Serum derived sIC from systemic lupus erythematosus (SLE) patients activate
829 human FcγR reporter cells. 25 patients and 4 healthy control individuals were separated into
830 three groups for measurement. A) Experiments shown for an exemplary group of 8 SLE
831 patients and two healthy individuals. Dose-dependent reactivity of FcγRs IIIA and IIB/C was
832 observed only for SLE patient sera and not for sera from healthy individuals. FcγRs I and IIA
833 show no reactivity towards clinical IC in line with previous observations. B) Activation of
834 FcγRs IIB/C and IIIA by patient serum is mediated by serum derived sICs. Patient serum
835 samples were depleted of sICs by PEG precipitation and the supernatant (SN) was compared
836 to untreated serum regarding FcγR activation (left). Performed in technical replicates. IgG
837 concentration in the precipitate (PC), supernatant (SN) or unfractionated serum respectively is
838 shown in the bar graph (right). IC precipitation did leave non-complexed IgG in the
839 supernatant. C) FcγRIIIA activation, but not FcγRIIB/C activation, significantly correlates
840 with known SLE disease markers. FcγR activation data from A was correlated to established
841 SLE disease markers (α-dsDNA levels indicated as IU/ml or C3d concentrations indicated as
842 mg/L). FcγR activation from a dose-response curve as in A was calculated as area under curve
843 (AUC) for each SLE patient (n=25) or healthy individual (n=4) and expressed as fold change
844 compared to the healthy control mean. SLE patients with α-dsDNA levels below 50 IU/ml
845 and C3d values below 6 mg/L were excluded. One-tailed Spearman's.
846
847

848 **Figure 7**

849

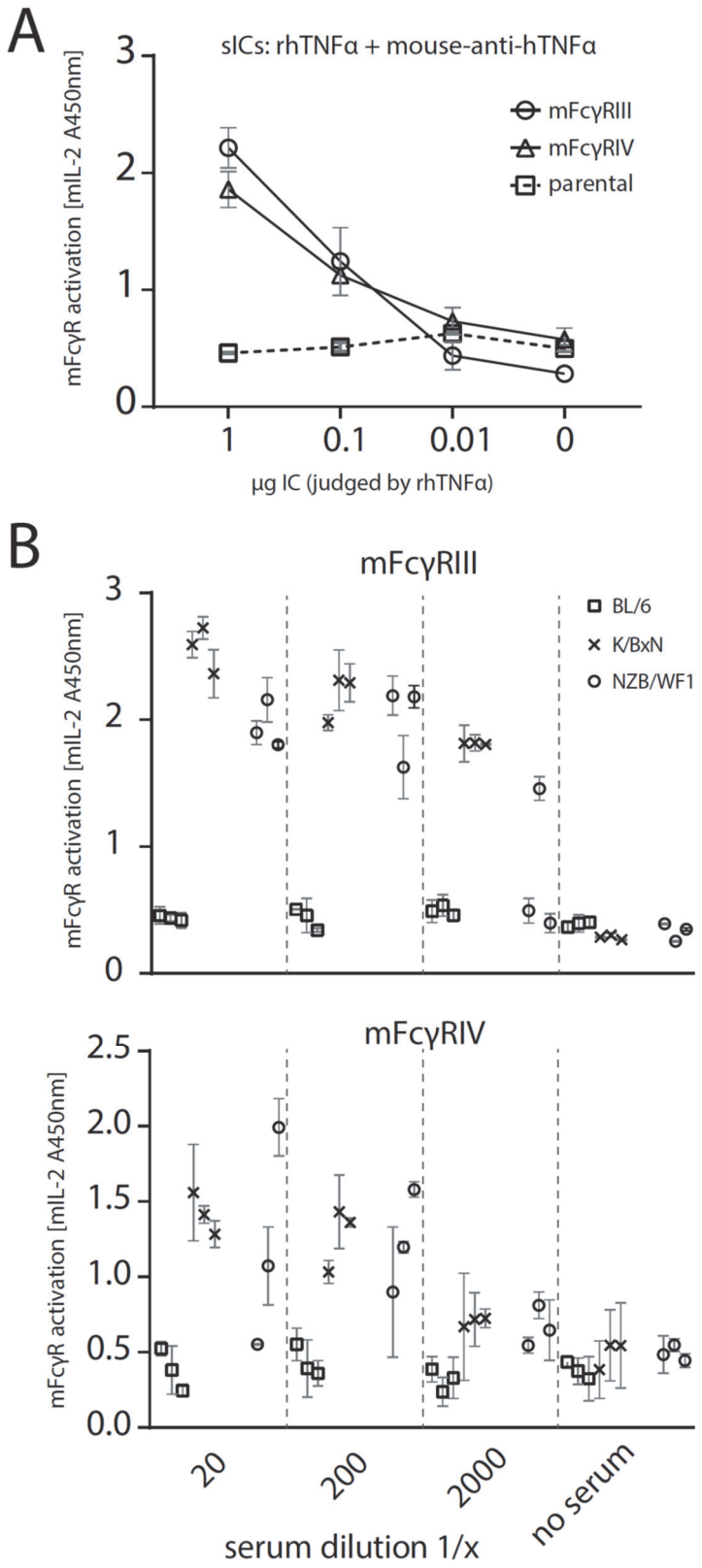

850

851

852 **Fig. 7. The reporter assay can be applied to mouse models of autoimmune disease.** A)
853 Reporter cells expressing mFcγRIII, mFcγRIV or parental BW5147 cells were incubated with
854 titrated amounts of synthetic sICs generated from rhTNFα and mouse-anti-hTNFα at a 1:1
855 ratio by mass. One experiment in technical replicates. Error bars = SD. B) Titrations of 3
856 mouse sera per group (C57BL/6, K/BxN or NZB/WF1) were incubated with mFcγR reporter
857 cells and FcγR activation was assessed as described above. Sera from BL/6 mice served as
858 negative control. Performed in technical replicates. Error bars = SD.
859
860

861 # -Supplementary Material-

862

863 **Figure S1**

864

865

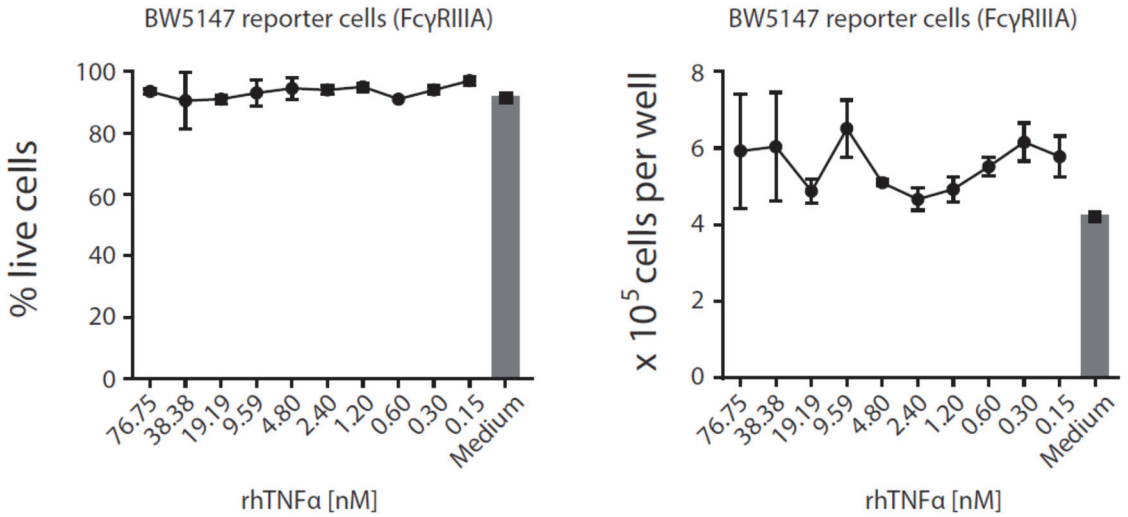

866

867 **Fig. S1. rhTNFα is not toxic to mouse lymphocyte BW5147 cells even at high**
868 **concentrations**. Cell count and percentage of live cells were unaltered over a 16 h time frame
869 of reporter cell culture in the presence of indicated rhTNFα concentrations and comparable to
870 regular growth in complete medium. Experiments were conducted in 3 replicates. Error bars =
871 SD.

872

873 **Figure S2**

874

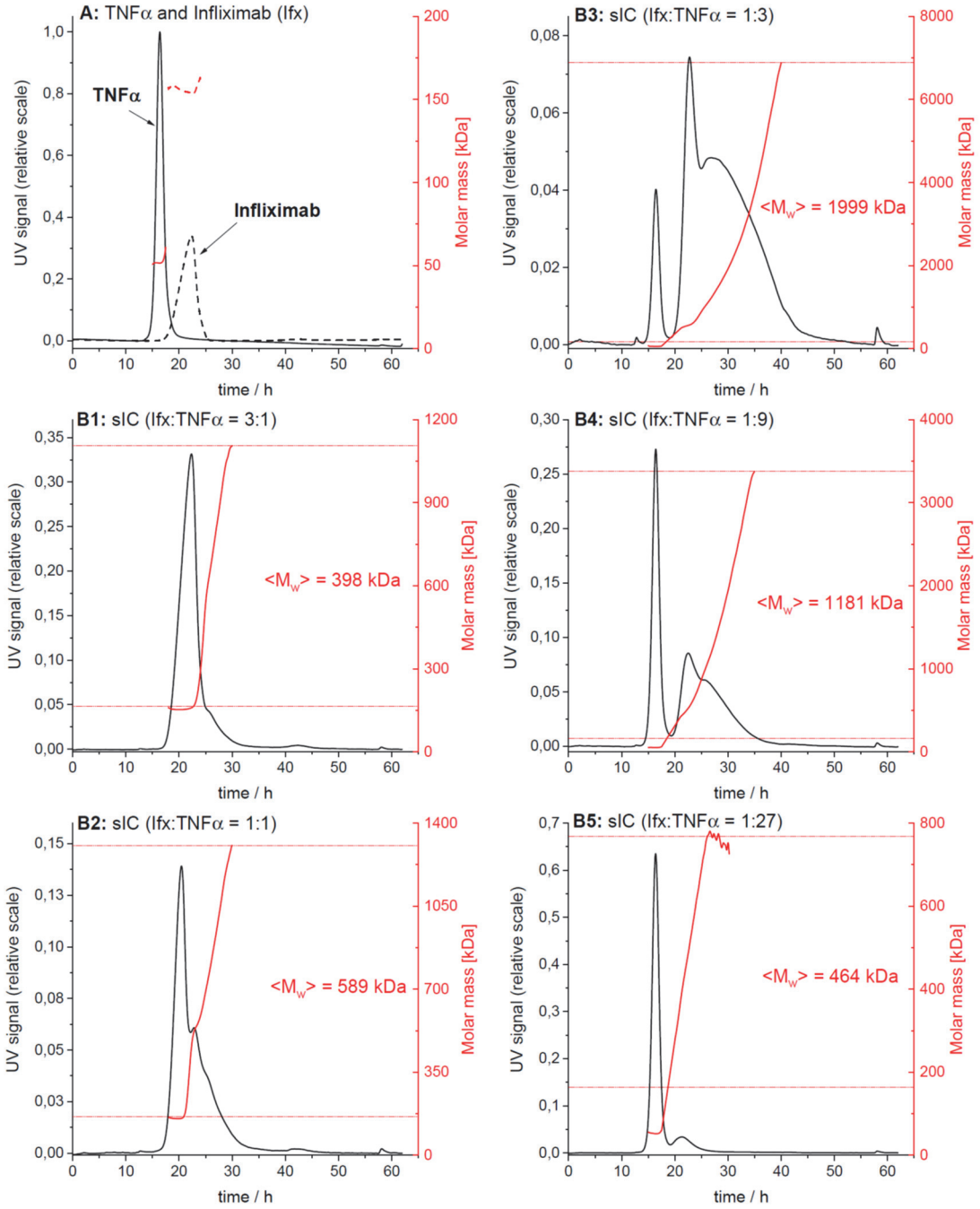

875

876

877 **Fig. S2. AF4 elution profiles of Ifx/TNFα-immune complexes.**

878 The elution profiles from one of three independent runs are shown. Protein concentration in
879 the eluate is shown in black (UV signal at λ = 280 nm, normalized to the highest UV signal
880 found in this experiment), molar masses determined by MALS for a given retention time in
881 red. Horizontal red lines indicate the range of molar masses used to calculate the mass-
882 weighted mean of molar masses $<M_w>$. A) Overlay of the elution profiles obtained for TNFα
883 and Ifx, respectively; B1 to B5) Elution profiles for sICs formed after incubation of TNFα and
884 Ifx at different molar ratios.

885

886 **Table S1**

Sample	Range of assigned molar masses [kDa]			Mass-weighted mean of assigned molar masses [kDa]			
	Run 1	Run 2	Run 3	Run 1	Run 2	Run 3	Mean ± SD
Infliximab, IFX	158 – 182	153 – 164	159 – 193	162	156	163	160 ± 4
TNF -alpha	52 – 55	51 – 61	52 – 62	52	52	52	52 ± 0
Immune complexes							
IFX/TNF 3:1	182 – $1.16 \cdot 10^3$	164 – $1.11 \cdot 10^3$	193 – $1.10 \cdot 10^3$	409	398	518	442 ± 66
IFX/TNF 1:1	182 – $2.06 \cdot 10^3$	164 – $1.31 \cdot 10^3$	193 – $1.42 \cdot 10^3$	801	589	681	690 ± 106
IFX/TNF 1:3	182 – $5.05 \cdot 10^3$	164 – $6.89 \cdot 10^3$	193 – $10.8 \cdot 10^3$	$1.77 \cdot 10^3$	$2.00 \cdot 10^3$	$2.61 \cdot 10^3$	$2.13 \cdot 10^3$ ± 435
IFX/TNF 1:9	182 – $5.36 \cdot 10^3$	164 – $3.38 \cdot 10^3$	193 – $3.51 \cdot 10^3$	$1.66 \cdot 10^3$	$1.18 \cdot 10^3$	$1.17 \cdot 10^3$	$1.34 \cdot 10^3$ ± 279
IFX/TNF 1:27	182 – $1.68 \cdot 10^3$	164 – 768	193 – $1.01 \cdot 10^3$	689	464	521	558 ± 117

887

888 **Table S1. Analysis of the molar mass distribution of ICs from AF4 data.**

889 For a given elution time, the AF4 profiles provide the concentration (UV) at which a given
890 molar mass (MALS) of a protein is present in the sample. The molar mass distribution of Ifx,
891 TNFα and their immune complexes (sICs) was obtained by plotting the cumulative frequency
892 as a function of molar mass. For a selected range of molar masses, a mass-weighted mean
893 value ($<M_w>$) was calculated. All detected molar masses were selected in the case of Ifx and
894 TNFα whereas only molar masses larger than the maximal molar mass found for Ifx were
895 assigned to sICs. The table shows the range of assigned molar masses and the calculated
896 $<M_w>$ for each AF4 run (n = 3).